

Single-Mode Operations of a Circular Free-Electron Laser

Takahide Mizuno, Takashi Otsuki, Tsutomu Ohshima, and Hirobumi Saito

Institute of Space and Astronautical Science, 3-1-1 Yoshinodai, Sagami-hara, Kanagawa, Japan

(Received 14 November 1995)

A circular free-electron laser (FEL) consists of a rotating electron beam and a circular wiggler for compactness. This paper presents the demonstration of a high power (3.6 MW), single-mode (mode purity of 99%) oscillation of a circular FEL with relatively high efficiency (4.6%). Although a circular FEL has an axial streaming electron velocity and a wide instability bandwidth due to its negative mass effect, one can control a single-mode oscillation at cutoff frequency. [S0031-9007(96)01092-7]

PACS numbers: 41.60.Cr, 52.75.Ms

In recent years, intensive researches have been conducted on a free-electron laser (FEL). It is pointed out that compact FELs are required for applications of FELs. For this purpose not only the accelerator but also the wiggler and the optical system have to be reduced in size. One of the basic concepts to realize compact beam devices is circulation of an electron beam with a magnetic field as well as circulation of an electromagnetic wave beam with a ring resonator. The examples include a "photon storage ring" [1] in the infrared and optical regions and a "large orbit gyrotron" [2] in the microwave region.

A novel type of FEL, a "circular FEL," which has a rotating electron beam and a circular wiggler for compactness, was proposed by Bekefi [3]. It should be noted that the size of our circular wiggler is about 14 cm in diameter and 20 cm in length. The circular FEL has been studied experimentally by MIT and the University of Maryland [4–6]. Theoretical studies [7,8] found that the negative mass instability mechanism of the rotating electron beam enhances the growth rate and increases the instability bandwidth of a circular FEL. In this paper, we report the first experimental results of single-mode operations of a circular FEL with a relatively high efficiency and a wide instability bandwidth.

A circular FEL consists of a rotating electron beam and a compact circular wiggler as shown in Fig. 1(a). The circular wiggler is composed of an azimuthally (θ) periodic radial (r) wiggler magnetic field in a coaxial waveguide. The electrons rotate in the θ direction under an axial (z) magnetic field B_{z0} with the perturbed wiggling velocity in the z direction. The rotating electrons couple with a TM_{pq} traveling mode along the θ direction through the axial (z) electric field of the radiation. Here p and q denote the azimuthal and the radial mode number, respectively.

The frequency ω_0 of the beam mode can be written as

$$\omega_0 = (p + N)\Omega_c/\gamma + (k_z v_{z0}), \quad (1)$$

where N , Ω_c , γ , k_z , and v_{z0} are the wiggler periodicity, the nonrelativistic electron cyclotron frequency, the Lorentz factor, the axial wave number of the radiation, and the axial streaming velocity of the electron, respectively.

When there is an axial streaming velocity v_{z0} , the wiggler field yields the wiggling velocity not only in the z direction (v_z) but also in the θ direction (v_θ). From Eq. (1), the electron bunching in a circular FEL is caused

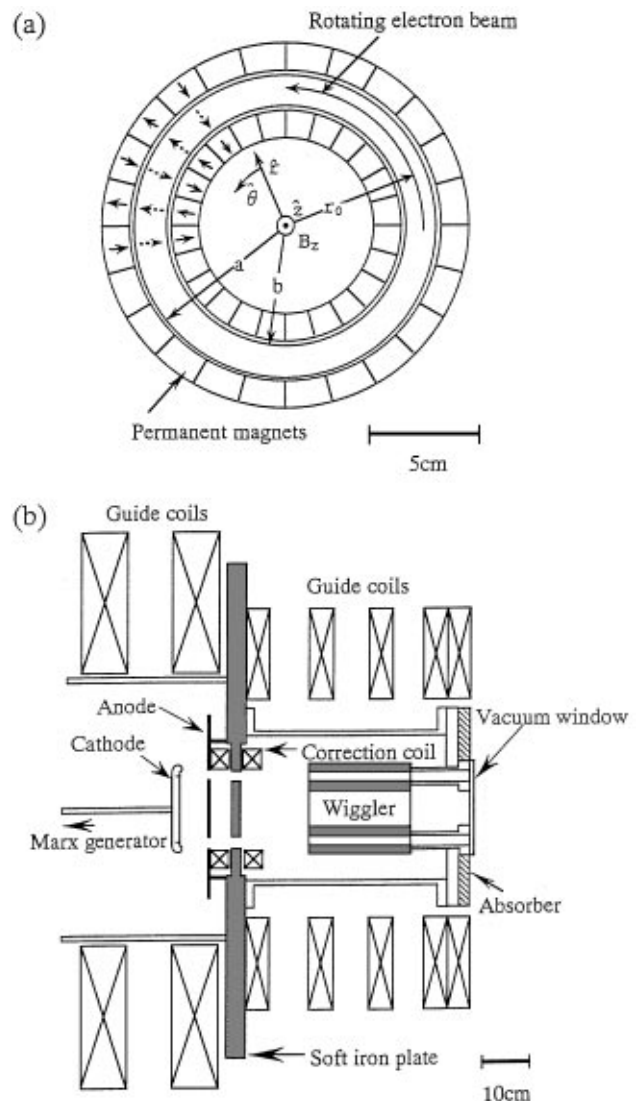


FIG. 1. Schematic diagram of circular free-electron laser. (a) Front view of circular wiggler, $N = 12$ wiggler periodicity, $a = 7.0$ cm, and $b = 5.5$ cm; (b) experimental apparatus.

by the energy change due to the $v_\theta E_\theta$ interaction and the $v_z E_z$ interaction, as well as the change of Doppler frequency $k_z v_{z0}$ due to the Lorentz force $v_\theta B_r$ in the z direction. Here E and B denote the electric and magnetic fields of the TM radiation. It is easily proven by Maxwell's equation for a TM mode that the first and third effect of the electron bunching have the opposite sign and are canceled out. Therefore electron bunching is caused only by the $v_z E_z$ FEL interaction, even though there is an axial streaming velocity. The cutoff TM radiation can have the most effective interaction in a circular FEL, since the cutoff TM radiation has only the z component E_z of the electric field. In addition, a cutoff TM radiation may have the highest cavity Q value in our open aperture cavity. Based upon these two facts, a circular FEL with an axial streaming velocity oscillates in a single mode at the cutoff ($k_z = 0$). This point is clearly demonstrated by our experiment.

The dispersion relation of the beam mode ω_0 in Eq. (1) and the TM_{pq} waveguide mode $\omega_s(p, q)$ is shown in Fig. 2 for the case of cutoff. The frequency detuning between the beam mode and the waveguide mode is defined as $\Delta\omega \equiv \omega_0 - \omega_s$.

A linear theory on a circular FEL was presented by Ref. [7]. The growth rate ω_i of the circular FEL radiation is given by the imaginary part of the propagation constant Γ from the following dispersion relation:

$$\Gamma^3 + 2\Delta\omega\Gamma^2 + \left[\Delta\omega^2 - \left(\omega_0 \frac{\Delta\gamma}{\gamma} \right)^2 + \frac{f_1 \omega_p^2}{\gamma} \right] \times \\ \Gamma = \frac{f_2 \omega_p^2 \omega_0 a_w^2}{4\gamma^3}, \quad (2)$$

where a_w , ω_p , and $\Delta\gamma$ are the normalized vector potential of the wiggler field, the plasma frequency, and the energy spread of the electron beam, respectively. The other variables are described in Ref. [7]. The dispersion relation of a linear FEL which consists of a linearly moving electron beam and a linear wiggler is as follows:

$$\Gamma^3 + 2\Delta\omega\Gamma^2 + \left[\Delta\omega^2 - \left(\omega_0 \frac{\Delta\gamma}{\gamma^3} \right)^2 - \frac{f_1 \omega_p^2}{\gamma} (1 + a_w^2) \right] \times \\ \Gamma = - \frac{f_2 \omega_p^2 \omega_0 a_w^2}{4\gamma^5} (1 + a_w^2). \quad (3)$$

A circular FEL [Eq. (2)] has a larger coupling term (the right-hand side) by a factor of γ^2 and a higher sensitivity to the energy spread than a conventional linear FEL [Eq. (3)]. Above all, the space charge term of a circular FEL [the fifth term of the left-hand side of Eq. (2)] has the opposite sign of the space charge term of a linear FEL in Eq. (3), resulting in the wide-band space charge instability. This wide-band instability is called a "negative mass instability" [9]. All these characteristics are caused by the negative mass effect of a rotating electron in a magnetic field. As a result, a circular FEL owns the unique properties caused by a coupling between the conventional FEL instability and the negative mass instability. Figure 3 shows the normalized growth rate

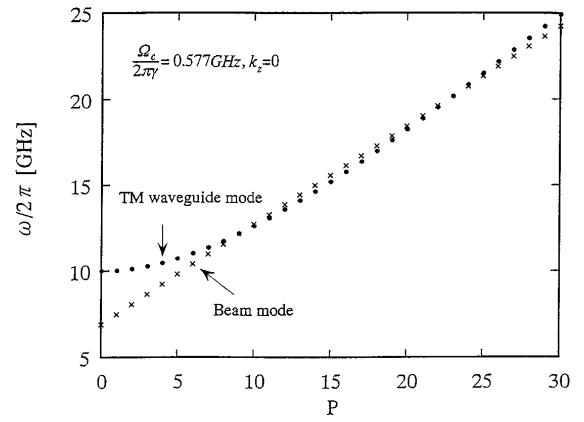


FIG. 2. Dispersion relation for cutoff TM waveguide mode ($k_z = 0$) and beam mode as a function of azimuthal harmonic number p , where $\gamma = 1.84$ (430 keV), $B_{z0} = 380$ G, and $\Omega_c/2\pi\gamma = 0.577$ GHz.

ω_i/ω_0 of a circular FEL as a function of the normalized detuning $\Delta\omega/\omega_0$. The parameters for the calculation are based on the experiment to be discussed in Fig. 4, where $\gamma = 1.84$, $a_w = 0.019$, $B_{z0} = 380$ G, $\omega_p/\omega_0 = 0.033$, $f_1 = 1$, and $f_2 = 2$. This figure indicates that a circular FEL has a wide permissible frequency detuning (an instability bandwidth) with a sensitive dependence on the energy spread.

A schematic configuration of our circular FEL oscillator experiment is shown in Fig. 1(b). The field emission cathode consisting of a hollow velvet cloth is directly energized by a Marx generator (<500 keV, $5 \mu s$). This hollow axially moving beam is converted to a large orbit rotating beam with a radius of $r_0 = 6.25$ cm and a width of 0.5 cm by passing through the cusped magnetic field. The compact circular wiggler is generated by permanent magnets embedded in the coaxial conductors (the inner radius $b = 5.5$ cm and the outer radius $a = 7.0$ cm) with $N = 12$ periodicity. The amplitude of the wiggler field B_w at the center of the gap is 900 G. The coaxial conductors

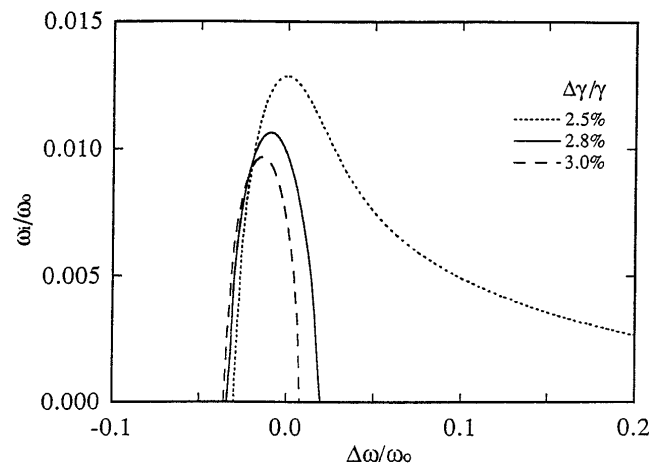


FIG. 3. Theoretical growth rate ω_i/ω_0 of circular FEL as a function of frequency detuning $\Delta\omega/\omega_0$, where $\gamma = 1.84$, $a_w = 0.019$, $B_{z0} = 380$ G, $\omega_p/\omega_0 = 0.033$, $f_1 = 1$, and $f_2 = 2$.

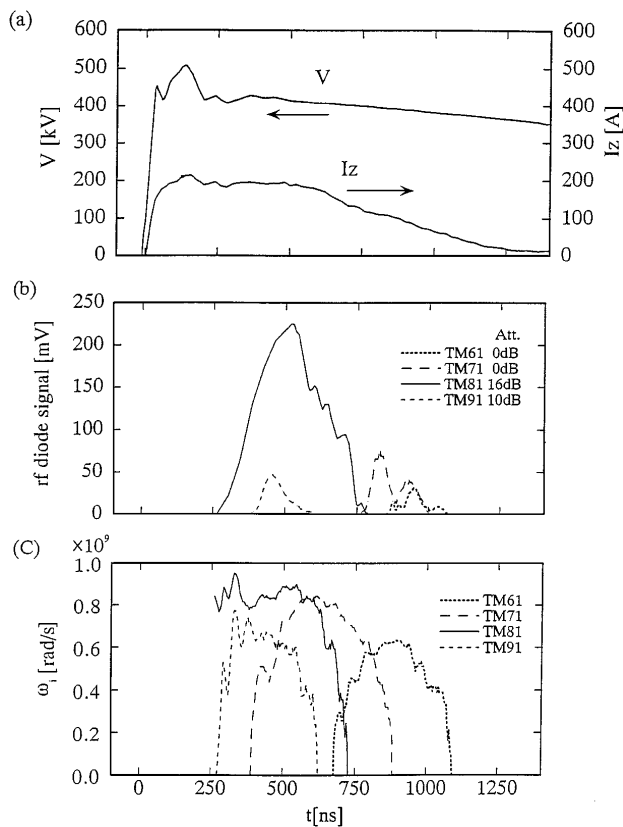


FIG. 4. Temporal profile of the oscillation. (a) Accelerating voltage V and beam current I_z . (b) rf diode signals of TM_{61} , TM_{71} , TM_{81} , and TM_{91} (12.18 GHz). The rf attenuation for the main TM_{81} mode and the spurious TM_{91} are 16 and 10 dB larger than the attenuations for TM_{61} and TM_{71} modes. (c) Theoretical growth rates where $\Delta\gamma/\gamma = 2.8\%$.

also act as a coaxial cavity with open apertures for the cutoff TM radiation of $k_z = 0$. The length (l) of the coaxial cavity is 35 cm, which includes the length $l_w = 20$ cm of the compact wiggler.

The far field radiation from the open aperture of the circular FEL is measured with standard gain (15 dB) horn antennas. The detector and the attenuator are carefully calibrated by HP power meters. It is theoretically predicted [10] that only TM modes (neither TE nor TEM) in coaxial waveguides irradiate their main lobe off axis. It is experimentally confirmed [11] that the measured far field has the main lobe off axis. In the circular wiggler, the TM traveling wave mode along the θ direction interacts with the rotating electron beam. Therefore the far field pattern is expected to be axially symmetric, which is also experimentally checked by scanning measurements in two (vertical and horizontal) planes.

The total output power is obtained by spatial integration using the experimentally measured intensity of the far field, based on the reasonable assumption of axial symmetry. The shot-by-shot reproducibility is as good as 3 dB for the power measurements. The rf field inside the cavity is measured with a tiny loop antenna (1 mm inner diam) at the inner surface of the cavity conductor. We obtain the

accurate frequency spectrum in Ku and Ka band by means of a fast Fourier transform (FFT) function (frequency resolution of 3.9 MHz) of the digital oscilloscope for IF signal after heterodyne detection. Temporal evolution of each radiation mode is obtained with the YIG tunable bandpass filter (10–40 GHz, 3 dB bandwidth of 30–40 MHz).

In Fig. 4(a), we display wave forms of the accelerating voltage V and the beam current I_z entering to the cavity measured by a Faraday cup under the axial guide magnetic field of $B_{z0} = 380$ G. The voltage gradually decreases from a flat top voltage of $V_0 = 430$ kV due to discharge of the Marx generator. While the main radiation mode is oscillating, the electron velocity ratio $\alpha (= v_{\theta 0}/v_{z0})$ is about 2–3. Here $v_{\theta 0}$ is a rotating velocity without wiggling motion.

Figure 4(b) shows the rf diode signals of the main TM_{81} mode at 11.77 GHz, the weak spurious modes of TM_{61} at 11.04 GHz, TM_{71} at 11.38 GHz, and TM_{91} at 12.18 GHz. Note that the spectrum spacing of each mode is about $\Delta f/f = 4\%$. The theoretical cutoff frequencies (i.e., $k_z = 0$) of the TM modes are 11.73 GHz for TM_{81} , 11.00 GHz for TM_{61} , 11.35 GHz for TM_{71} , and 12.14 GHz for TM_{91} , respectively. The measured frequencies are in good agreement with the theoretical cutoff frequencies within an accuracy of 0.4%, which may be caused by mechanical accuracy of the coaxial waveguide. The FFT measurements indicate that the rf signal of each mode has a very narrow frequency spectrum width of $\Delta f/f = 0.1\%$. These experimental results make it clear that a circular FEL oscillates at cut off, even though there is an axial streaming electron velocity.

The peak power of the spurious modes of TM_{61} , TM_{71} , and TM_{91} are 31, 25, and 20 dB lower than the main TM_{81} mode, respectively. From these experimental results, the main TM_{81} mode is considered a single mode oscillation with a mode purity of 99%.

In this single mode operation of the TM_{81} mode, the output power radiating from one of two open end apertures of the coaxial cavity is 600 kW. Since the frequency measurement indicates that the radiation mode is cut off (i.e., $k_z = 0$), equal amounts of power radiate symmetrically from both of the open end apertures of the cavity due to diffraction [12]. Based on the rf measurement inside the cavity by means of the loop antenna, we calculated the storage rf energy U of 6.2 mJ. Therefore, the quality factor Q of the cavity for the TM_{81} mode can be estimated to be 400.

We compare these experimental results with the linear theory of the circular FEL [7]. Figure 4(c) illustrates theoretical curves for the growth rate ω_i/ω_0 versus time. These growth rates are calculated with Eq. (2), combined with the time-dependent experimental data of the electron beam shown in Fig. 4(a). The electron density is obtained with the measured axial current I_z and the velocity ratio $\alpha = v_{\theta 0}/v_{z0}$ given by the theoretical expression in [13]. The energy spread of the beam from the velvet field emission cathode similar to ours was measured to

be $\Delta\gamma/\gamma = (2-3)\%$ by Japan Atomic Energy Research Institute [14]. In our analysis, the energy spread of the beam is assumed to be $\Delta\gamma/\gamma = 2.8\%$. The cavity decay time $\tau_d (= Q/\omega_s = 5.4$ ns) and the radiation rise time $\tau_r [= (2\omega_i l_w/l - \omega_s/Q)^{-1} = 1$ ns] are negligibly short compared with the observed rf pulse width of 500 ns.

The first indication that the TM_{81} mode has the highest growth rate from the beginning of the voltage flat top ($t = 300$ ns) and then decreases with decreasing the voltage is shown in Fig. 4(c). This theoretical result suggests that the TM_{81} mode radiation dominates over the TM_{91} and TM_{71} modes from the beginning of the voltage flat top ($t = 300$ ns) for the initial voltage of $V_0 = 430$ kV. This theoretical prediction is in agreement with the experimental result shown in Fig. 4(b). A second observation of Fig. 4(c) is that after $t = 600$ ns the growth rate of the TM_{71} mode becomes highest instead of the TM_{81} mode. However, the experimental result of Fig. 4(b) shows that the TM_{71} mode starts to oscillate at $t = 780$ ns when the main TM_{81} mode stops oscillation. The TM_{71} mode is completely suppressed during the preceding oscillation of the TM_{81} mode.

The oscillating mode TM_{pq} is determined by the dispersion diagram shown in Fig. 2. We clearly observed the mode jump as the electron energy was changed. As discussed in Fig. 4, the TM_{81} mode is a main oscillation mode for $V_0 = 430$ kV. When we decreased the initial flat top voltage to $V_0 = 400$ kV, the TM_{71} mode replaced the TM_{81} mode as a single oscillation mode.

We discuss here the permissible frequency detuning as well as the spurious modes. As seen in the results of Figs. 4(a) and 4(b), the electron energy decreases by 9.8% (from 430 to 388 keV) during the main TM_{81} radiation pulse. As a result, we estimate the permissible frequency detuning $\Delta\omega/\omega_0$ of about 5% for the TM_{81} mode oscillation, using Eq. (1). This observed value of the permissible frequency detuning is in good agreement with the theoretical value of 5% in Fig. 3 for an energy spread of $\Delta\gamma/\gamma = 2.8\%$, [14]. This agreement indicates that the wide permissible frequency detuning is caused by the negative mass effect of a circular FEL [7].

As seen in the frequency measurement, the frequency spacing of the TM_{p1} modes is about 4%. The frequency spacing of the beam modes, Eq. (1), is about 5%. These frequency spacings are comparable with the permissible frequency detuning (5% for the TM_{81} mode). Therefore, the beam mode could couple with a single mode or simultaneously with a few modes of the waveguide TM_{p1} radiation, depending on the experimental condition (see Fig. 2). This feature is the cause of our spurious modes.

In order to suppress these competing modes, we formed a narrow shape of the rotating electron beam by means of a narrow cusped magnetic field [13] and optimized the accelerating voltage as well as the axial magnetic field. We experimentally demonstrated the single-mode TM_{81} oscillation with a mode purity of 99%.

The maximum output power of the TM_{81} main mode that we observed from the one open end aperture of the circular FEL cavity is 1.8 MW for $V_0 = 412$ kV and $B_{z0} = 370$ G. We evaluate the energy efficiency from the electron kinetic power ($I_z V$) to the total radiation power P_{out} diffracted from both the two open end apertures (i.e., 1.8 MW $\times 2 = 3.6$ MW). It should be noted that the radiation is cut off (i.e., $k_z = 0$) and equal amounts of the power radiate symmetrically from both sides [12]. The total energy efficiency is found to be 4.6%.

In conclusion operations of a high power single-mode oscillation of a compact circular FEL with relatively high efficiency are demonstrated. It is experimentally shown that a circular FEL oscillates as a monochromatic ($\Delta f/f = 0.1\%$), single mode TM_{81} (the mode purity of 99%) at cut off, even though there is an axial streaming velocity of the electron beam. The linear theory predicted that a circular FEL has a wide instability bandwidth due to its negative mass effect. This feature is experimentally confirmed for the single mode oscillation by the observed large permissible detuning. These results give encouragement to further develop a circular FEL as a compact FEL.

We wish to thank Jonathan S. Wurtele and George Bekefi for useful discussions.

-
- [1] H. Yamada and H. Tsutsui, Nucl. Instrum. Methods Phys. Res., Sect. A **331**, 566 (1993).
 - [2] W. Lawson and C.D. Striffler, Phys. Fluids **28**, 2868 (1986).
 - [3] G. Bekefi, Appl. Phys. Lett. **40**, 578 (1982).
 - [4] W.W. Destler, F.M. Aghamit, D.A. Boyd, G. Bekefi, R.E. Shefer, and Y.Z. Yin, Phys. Fluids **28**, 1962 (1985).
 - [5] F. Hartmann and G. Bekefi, Phys. Fluids **30**, 3283 (1987).
 - [6] R. Chojnacki and W.W. Destler, IEEE J. Quantum Electron. **23**, 1605 (1987).
 - [7] H. Saito and J.S. Wurtele, Phys. Fluids **30**, 2209 (1987).
 - [8] Y. Kawai, H. Saito, and J.S. Wurtele, Phys. Fluids B **3**, 1485 (1991).
 - [9] R.J. Brigg and V.K. Neil, Plasma Phys. **9**, 209 (1967).
 - [10] E.A. Wolff, *Antenna Analysis* (Artech House, Norwood, Massachusetts, 1988), Sec. 5.10.
 - [11] T. Mizuno, T. Ohtsuki, T. Ohshima, and H. Saito, Nucl. Instrum. Methods Phys. Res., Sect. A **358**, 131 (1995).
 - [12] Even if k_z were finite, $ck_z/\omega_s \leq 0.08$ is estimated by a discrepancy between the measured oscillating frequency (11.77 GHz) and the cutoff frequency (11.73 GHz) of the waveguide. The unbalance of the radiating powers from the front aperture and the back aperture can be calculated to be less than about 1.7 dB in the case of $ck_z/\omega_s \leq 0.08$, according to Ref. [14].
 - [13] M.J. Rhee and W.W. Destler, Phys. Fluids **17**, 1574 (1974).
 - [14] M. Takahashi, S. Kawasaki, K. Sakamoto, A. Watanabe, Y. Kishimoto, and M. Shiho, Japan Atomic Energy Research Institute Report No. JAERI-M 94-048, 1994.